Remote Sensing Solutions, Inc.

PROJECT: Operational SFMR-NAWIPS Airborne Processing and Data Distribution Products

NOAA Award No.: NA05OAR4171101

Performance Report Number: 01

Prepared By: Dr. James Carswell

Date: 03/01/2006

1. 0 SCOPE

This document summarizes the work performed and accomplishments achieved to date for the Joint Hurricane Testbed (JHT) project entitled, "Operational SFMR-NAWIPS Airborne Processing and Data Distribution Products."

2.0 WORK PERFORMED

In accordance with the approved schedule for this JHT project, the focus during this first interim period was: 1) to develop and document an automatic calibration tuning algorithm for the AOC SFMR instrument, and 2) to develop real-time and post comparison tools. These efforts were to use the AOC SFMR data collected during the 2005 hurricane season. Significant delays in receiving these data have delayed our efforts on the JHT project to some extent. However, more than eighty percent of the calibration algorithm development is completed and seventy percent of the software has been developed and tested. At the end of this report, an adjusted project plan is given; detailing a schedule that will bring this project in line with the original time table (Table 2). Steps have been taken to ensure calibration and validation results are available prior to the Interdepartmental Hurricane Conference (IHC), which will be held on 20-24 March 2006. Dr. Carswell will be presenting at the IHC. Additionally, an opportunity was made available through the efforts of Drs. Carswell and Chang and with help from NOAA AOC crew to execute specific flight patterns during the 2006 Ocean Winds Winter Experiment to address installation and antenna pattern issues that were detected during the 2005 hurricane season. Below, these activities and the progress made to date are summarized.

2.1 Automatic SFMR Calibration Tuning

The absolute calibration of the AOC SFMR is critical for obtaining reliable and accurate wind and rain retrievals. Traditional radiometric calibration approaches for microwave radiometers often observe one or more targets with known brightness temperatures – referred herein as calibration loads. Typical loads range from man-made loads consisting of microwave absorber at different physical temperatures to natural targets such as the sky (clear day). Often, the internal temperature of the instrument is also varied during these measurements to correlate gain changes to internal temperature changes of the instrument and antenna feed. Although such approaches can produce very accurate brightness temperature measurements, significant changes in the environmental and physical conditions between calibration and operations can lesson the accuracies. For example, conducting material near the antenna aperture may change the reflective losses of the antenna. This is believed to have occurred with the AOC SFMR during the 2005 hurricane season. Furthermore, model functions that relate geophysical parameters with brightness temperature can have small errors or biases. Often satellite-based sensors use targets such as rain forests or other land or ocean targets to remove or tune the calibration,

which removes biases between the measurements and the model function. In the case of the AOC SFMR, we believe that some of these conditions exist, and through this JHT effort an automated, in-flight calibration approach has been developed to automatically compensate for these limitations. Note that previously, SFMR calibration was solely performed through lab-based testing prior to each experiment season and than the calibration numbers were adjusted manually based on test flights.

Figure 1 presents an over simplified block diagram of the AOC SFMR. Because of the restrictions placed on proprietary information of ProSensing, Inc, a detailed block diagram was unavailable. With these restrictions, Remote Sensing Solutions, Inc. (RSS) could neither obtain nor present such a diagram in this report. Nevertheless, for this discussion the simplified diagram shown below should more than suffice. To understand the automatic calibration "tuning" algorithm, the manner in which this instrument acquires its measurements is reviewed.

There are two types of calibrations: internal and external. The internal calibration measures the gain transfer function of the instrument. The gain transfer function relates the voltages at the Dicke switch to those outputted by the detection board. By measuring this function and monitoring changes in it, the final estimate of the scene brightness temperature is not affected by fluctuations in the gain transfer function.

In the AOC SFMR, this is accomplished using a reference and internal calibration load that are attached to the Dicke switch. The internal calibration load for this instrument was initially a hot load (noise diode) but was replaced with a cold load (cold FET) during the 2005 season. For this reason it is referred to as the internal cold/hot load. Both this load and the reference load have a stable and known noise emission (or brightness temperature). The Dicke switch periodically selects one of these loads and the output voltage of the instrument is recorded (i.e. V_{ical} and V_{ref}). By monitoring the difference between these two voltages, changes in the internal gain transfer function can be measured and then corrected for in the processing algorithm that derives the brightness temperature of the scene.

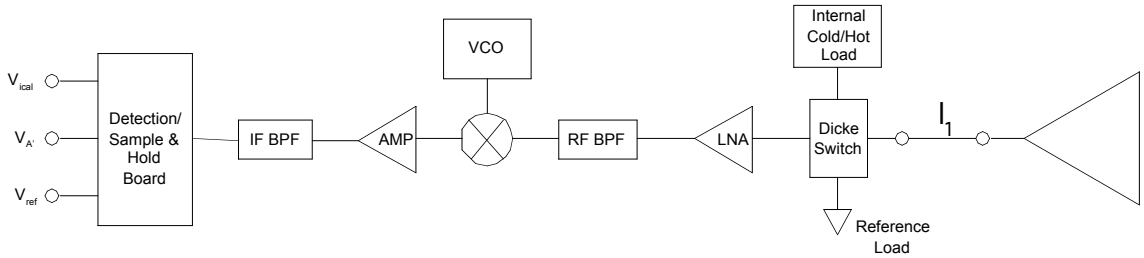

Figure 1: Simplified AOC SFMR block diagram (VCO steps through six frequencies that allows the SFMR to make measurements at six different RF frequencies from 4.74 to 7.09 GHz.

The external calibration, which is often referred to as the calibration of the instrument, accounts for the reflective and absorptive losses in the antenna system. Before stepping through the external calibration process, it is important to understand how this system measures the scene brightness temperature.

During operation, the three voltages shown in Figure 1 are measured. Most likely a sample and hold circuit is used in the detection board such that these voltages are low pass filtered and held synchronously with the switching of the Dicke switch and then sampled by an analog to digital converter. That is, when the Dicke switch connects the antenna feed to the receive chain, the signal is amplified, down converted, filtered, and detected to produce the voltage $V_{A'}$ or its digital representation (i.e. ADC output bits). In this manner, $V_{A'}$ represents the scene emission incident on the antenna reduced by the absorptive and reflective losses of the antenna and antenna feed, plus the noise contribution of the antenna feed and antenna that comes from their absorptive losses, the summation is then multiplied by the gain transfer function of the instrument. By switching between the antenna feed, reference load and the internal cold/hot load, at rates much faster than changes in the gain transfer function, and measuring / calculating the difference signal (i.e. $V_{A'} - Vr_{ef}$, $V_{ical} - V_{ref}$), the effects of these gain transfer function changes are minimized and can be accounted for. Further, the noise contribution from the receiver components, such as the amplifiers, is the same irregardless of the Dicke switch position and therefore disappears in the difference. The only unknown at this stage is the absorptive and reflective losses of the antenna system. Thus, the external calibration process aims to account for these losses.

The calibration approach that we developed as part of this effort attempts to calibrate the instrument to the model function while installed on the aircraft. Taking advantage of the model function's insensitivity to low through moderate winds (< 30 kt), this approach can be automated to minimize requirements on the operator. Furthermore, this approach is designed to place minimal constraints on the mission in order that it can be performed routinely and/or as the opportunity or need arises. Note that the calibration is not expected to drift throughout the experiment season. However, the capability to periodically perform the calibration offers end users a higher level of confidence in the data.

For a Hach-Dicke mode radiometer, the scene brightness temperature (T_b), neglecting the absorptive losses of the antenna (at first), can be expressed as:

$$T_b = \left(\frac{V_A - V_{ref}}{V_{ical} - V_{ref}} \right) \left(K - T_{ref} \right) + T_{ref} \qquad (1)$$

where T_{ref} is the physical temperature of the reference load and K is the calibration coefficient. V_A, V_{ref} and V_{ical} are the detected signals shown in Figure 1. Note that this equation only contains a gain number for the calibration, and it is this feature that will enable us to derive the calibration from a single calibration

load (i.e. the ocean surface at low / moderate wind speeds). Solving for the calibration number, *K* can be expressed as:

$$K = \left(\frac{V_{ical} - V_{ref}}{V_A - V_{ref}} \right) \left(T_b - T_{ref} \right) + T_{ref} \qquad (2)$$

From equation (2), the only unknowns are the calibration number, *K*, and the scene brightness temperature, T_b. This means that if T_b is known, the calibration number can be derived directly from the measurements.

Figure 2 plots the ocean surface brightness temperature as a function of the ocean surface wind speed at 10 m altitude. The green curve is for 7.09 GHz and the red curve is for 4.74 GHz (upper and lower channels of the AOC SFMR). As this figure clearly shows, the brightness temperature is not very sensitive to the wind speed for low to moderate wind speeds (less than 30 knots). By deploying a GPS dropsonde to measure the winds or even simply extrapolating the flight level wind speed, a reasonable estimate of the brightness temperature can be made (within 0.1 Kelvin). The only other parameter value needed is the sea surface temperature (SST). Given that the SST is known (e.g. available from embedded SST maps), then under these conditions (which occur often), the brightness temperature can be estimated using the retrieval brightness temperature model. Using equation (2), the calibration coefficient can then be determined. Not only does this allow the calibration coefficient to be automatically determined during any flight, but it also automatically tunes to the model function so that any biases in the model function are immediately accounted for. Furthermore, the brightness temperature is least sensitive to wind speed during the occurrence of low wind speeds, and therefore to minimize retrieval errors caused by calibration errors, it is important to tune the calibration at low to moderate wind speeds. A 0.5 Kelvin difference at 10 kt can produce a 6 knot error whereas the same calibration error at 70 kt produces only a 0.7 knot error.

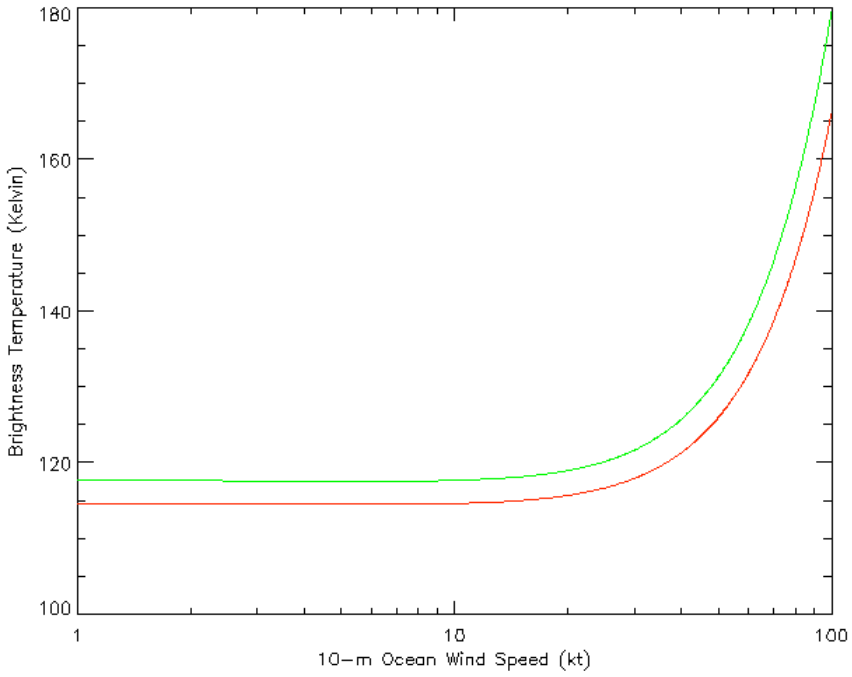

Figure 2: Ocean surface brightness temperature plotted versus 10-m wind speed (green - 7.09 GHz, red - 4.74 GHz)

To demonstrate the performance of this technique and its potential for operational use, equation (2) was applied to data obtained with the AOC SFMR during a test flight on 29 June 2005. In this case, the only information used to derive the calibration coefficient for each channel is the flight level data (i.e. altitude, flight level wind speed, flight level ambient temperature). The modeled Tb values were calculated using these flight level data and the SFMR Tb model function. No surface wind measurements were used. The SST was assumed to be 28 deg Celsius. The only filtering applied to the data is the removal of points where the pitch deviated by more than 3 degrees from the mean and the absolute value of the roll was greater than 3 degrees. Figure 3 plots the altitude, flight level wind speed and the flight level ambient temperature. During this time, the aircraft flew at several different altitudes experiencing different ambient temperatures and the flight level winds fluctuated from 2 to 7 m/s. Figure 4 plots the derived calibration number (K) for each channel. With the exception of the 5.31 GHz channel which experienced some anomalies at the beginning of this data record (potentially interference), the calibration numbers have a standard deviation of less than 2 deg. In practice, averaging would be implemented and the standard deviation after averaging would be reduced by a factor of ten or more. Neither surface wind measurements nor SST measurements (or table) were inputted, which resulted in additional noise. Despite these factors, the numbers appear to be very stable. Furthermore, these values show no dependence on altitude / ambient air temperature or flight level wind speed. If the absorptive losses in the antenna system were significant, the measured antenna temperature (or brightness temperature) would have varied with the ambient

temperature. There is no noticeable variation (correlation coefficient between the calibration number and the ambient temperature was 0.2 percent). Therefore, equation (2) is valid without needing to add in a correction for the absorptive losses.

Since there is no dependence on the flight level wind speed and the calibration numbers are essentially flat, the premise that one can use the ocean surface at low to moderate wind speeds as a calibration target seems valid. This is very significant. Currently, ProSensing, Inc. performs an elaborate laboratory calibration of the AOC SFMR. Their traditional calibration procedure results in a calibration equation with several coefficients and an offset. The offset comes from the fact that they perform a correlation analysis to relate internal temperature changes to changes in the output voltage. This process introduces an offset that otherwise should not be present. It also requires that multiple calibration targets be used to solve for both the gain and offset values. Even more important, this calibration approach does not take into account the effects of the aircraft on the reflective losses of the antenna nor any differences or biases with the model function used to retrieve the wind and rain from the SFMR measurements. The approach proposed here can be implemented with virtually no impact to operations, would essentially cost nothing to perform, can be performed during almost any flight since low to moderate wind speeds are almost always encountered and provides a true calibration of the instrument to the model function.

As of this week, RSS has received GPS dropsonde data for the 2005 hurricane season flights. We have produced a collocated SST data set from satellite, buoy and AXBT data. We have created a full archive of the raw AOC SFMR data set. Over the next two weeks we will run this auto calibration procedure on a subset of this collocated data set. The results will then be applied to the data not used to derive the calibration numbers. Wind speed and rain rate retrievals will be derived and compared against the GPS dropsonde surface wind estimates.

In addition to the GPS dropsonde data, we have continuous collocated scatterometer data at C and Ku-band from the IWRAP instrument. We are currently processing these data (7 terabytes) and will derive the oceans surface winds using a high wind speed scatterometer retrieval algorithm. Since IWRAP directly measures precipitation along its beam, we can remove the rain contaminated data with 100 percent accuracy so that this does not bias our scatterometer wind estimates. Since the footprint of IWRAP and SFMR are collocated, and since the measurements are continuous, this collocated data set will provide the best possible validation of the AOC SFMR calibration and retrievals. We expect to complete this analysis within the next two months

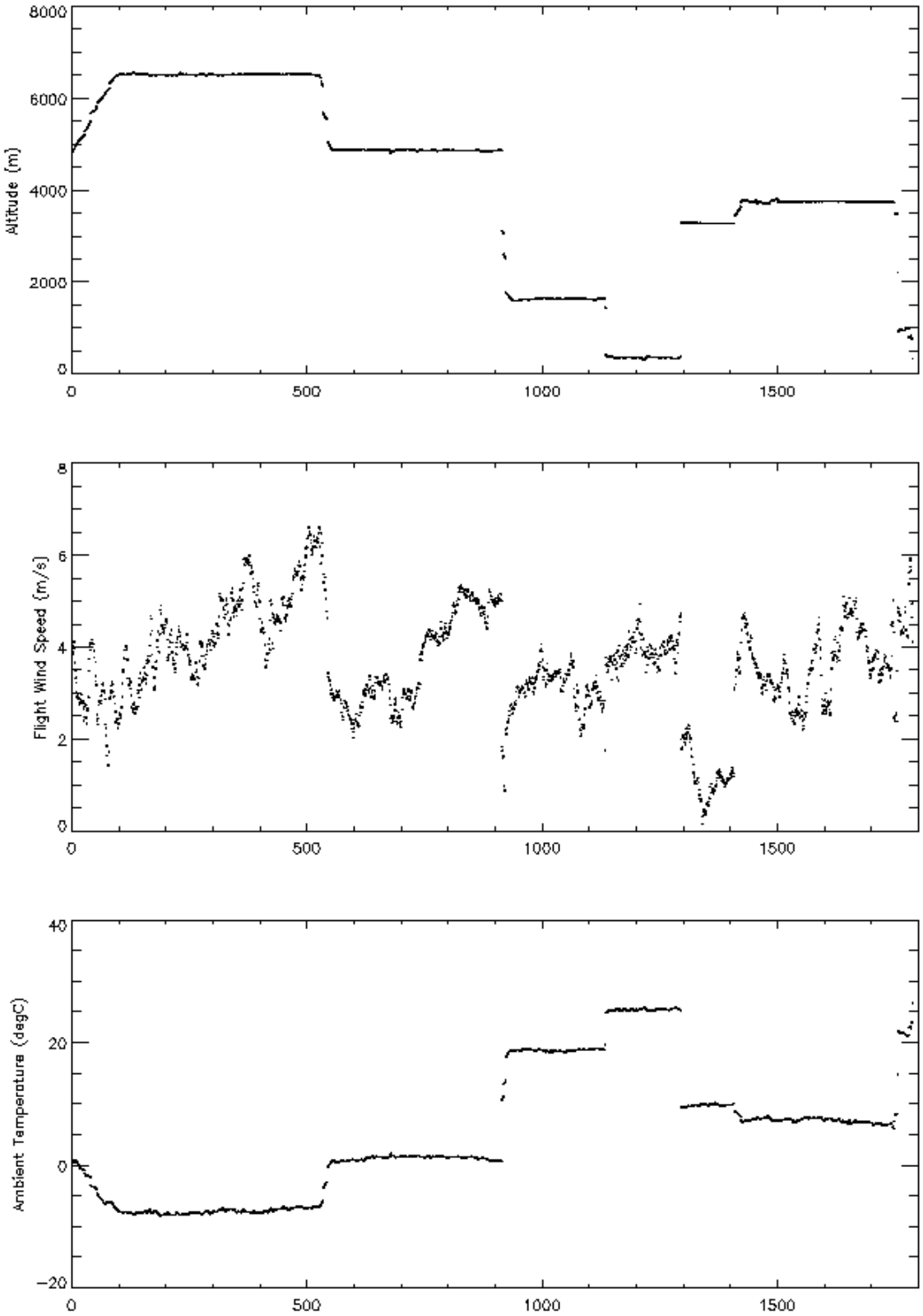

Figure 3: The altitude, flight level wind speed and ambient air temperature for the mission on 29 June 2006 are plotted.

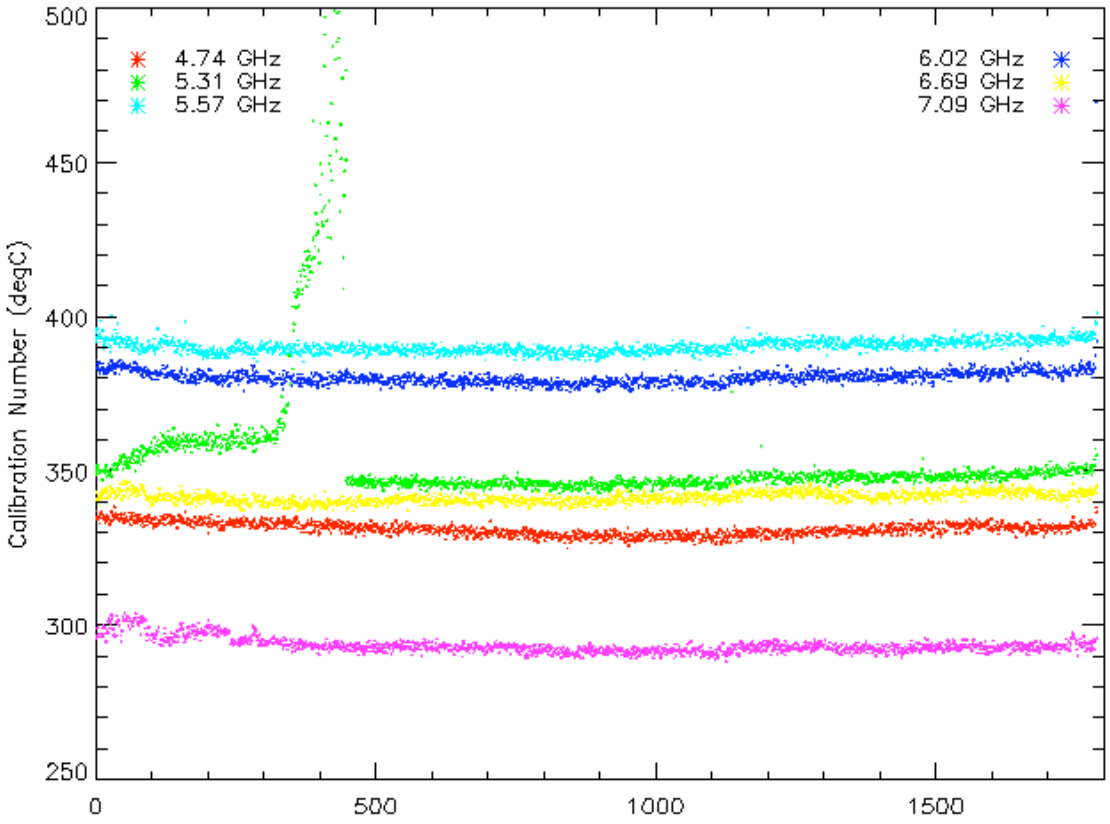

Figure 4: AOC SFMR calibration numbers (*K*) derived from the raw data on 29 June 2005 using the auto calibration procedure.

2.2 Comparison Tools

An initial set of libraries, functions and procedures have been developed to collocate and compare AOC SFMR retrievals with GPS dropsondes. RSS is currently working on a client/server system for NOAA/NESDIS that will provide these data in real-time over the internet. As such, the comparison tools that we are developing will also be made compatible with these real-time data feeds so that comparisons can be run live on the aircraft, and also on the ground at NHC and at HRD. Since we only recently received all the data required for the comparisons, these software tools have not been completed. We expect to complete them over the next two months. Initial comparisons will be presented during the IHC.

As part of this effort, we are constructing a full data archive of the AOC SFMR data, collocated SST measurements, GPS dropsonde ocean surface wind estimates and IWRAP surface winds and rain estimates. **Table 1** lists the flights that will be included in the archive. Note that IWRAP data is only available for N42RF missions, denoted by an 'H' following the Mission ID, from September since it had not been installed in the aircraft until the end of August. This data

archive will be made available by request and will server as the central repository for all algorithm development and testing.

Table 1: Data Archive - Flights

Mission ID	SFMR ID	Description
20050629H	US002	Calibration Mission
20050629I	US001	Cal.
20050703H	US002	Ferry
20050703I	US001	Ferry
20050705H	US002	Cindy
20050705I	US001	Dennis
20050706I	US001	Dennis
20050708H	US002	Dennis
20050709H	US002	Dennis
20050709I	US001	Dennis
20050710H	US002	Dennis
20050710I	US001	Dennis
20050711H	US002	Emily
20050713I	US001	IFEX
20050714H	US002	IFEX
20050715H	US002	IFEX
20050715I	US001	IFEX
20050716H	US002	IFEX
20050716I	US001	IFEX
20050717H	US002	Ferry
20050718I	US001	Emily
20050722I	US001	Gert
20050723H	US002	Gert
20050724I	US001	Gert
20050724I2	US001	Gert
20050817I	US003	Cal.

(Table 1 cont.)

Mission ID	SFMR ID	Description
20050822I	US003	Cal.
20050823I	US003	Cal.
20050825I	US003	Katrina
20050827I	US003	Katrina
20050828I	US003	Katrina
20050829I	US003	Katrina
20050906H	US002	Ophelia
20050907H	US002	Ophelia
20050907I	US003	Ophelia
20050908I	US003	Ophelia
20050909H	US002	Ophelia
20050909I	US003	Ophelia
20050911H	US002	Ophelia
20050911I	US003	Ophelia
20050912H	US002	Ophelia
20050913H	US002	Ophelia
20050916H	US002	Ophelia
20050917H	US002	Ophelia
20050918I	US003	IFEX
20050919I	US003	Rita
20050920I	US003	Rita
20050921I	US003	Rita
20050922H	US002	Rita
20050922I	US003	Rita
20050923H	US002	Rita
20050923I	US003	Rita
20050926I	US003	Post-Rita

(Table 1 cont.)

Mission ID	SFMR ID	Description
20051020H	US002	Wilma
20051022H	US002	Wilma
20051023H	US002	Wilma

2.3 RFI / Land Quality Control

Identifying, flagging and/or removing contamination due to radio frequency interference (RFI) and land features within the AOC SFMR field of view is essential, especially for hurricane land falling missions. To properly develop algorithms and land masks, accurate knowledge of the antenna pattern is required. Initially we requested this information from NOAA AOC who directed us to ProSensing. Once again, due to the fact that this information was considered proprietary, we could not use it for this effort. Furthermore, changes to the aircraft pod are believed to affect the antenna pattern of the AOC SFMR, and therefore the ProSensing antenna patterns would not be accurate.

To overcome this problem, we developed a plan to directly measure the patterns. By operating the SFMR over a discrete water / land boundary, the brightness temperature is a unique step function. The measured brightness temperature then becomes a convolution of this unit step function and the antenna pattern. Since the AOC SFMR requires approximately four seconds to step through all six of its channels, the aircraft flight track cannot be perpendicular to the boundary because the transition would be under sampled. A simulator was developed to model the AOC SFMR sampling and flight track. From this simulator, a flight track was derived based on aircraft ground speed and altitude to ensure a minimum of six samples per track per channel would be acquired. The attack angle is varied to provide enough samples. As the aircraft altitude decreases, the SFMR footprint decreases. To gather enough samples of the transition, the aircraft then needs to fly more parallel to the boundary. Using this code, several flight patterns were developed and executed during the Ocean Winds Winter Experiment that was based out of Anchorage, Alaska. These data will be processed over the next two months and the antenna pattern derived.

From the derived antenna pattern, the land interference radius will be determined and used to specify the requirements for the land mask algorithm. The patterns will also be used to simulate potential RFI sources to gain an understanding to the extent they may affect the measurements and to develop RFI detection routines.

Table 2: Revised Project Schedule

Task #	Task Descriptions	Completion Date	Deliverable
1	Time Table for Year 1	8/26/2005	Document describing schedule of tasks and deliverables for year 1.
2	Project Requirements Review	9/23/2005	Project Requirements Document
3	Calibration Tuning Algorithm	11/18/2005	Calibration tuning algorithm and validation results.
4	Real-time & Post Comparison Tools.	4/28/2005	Procedures and source code that compares SFMR, GPS dropsonde and other surface wind speed estimates in real-time and/or post processing.
5	Automated SFMR Calibration Tuning	4/28/2006	Software, procedures and documentation for automated SFMR calibration tuning and validation.
6	Interim Report	2/28/2006	Interim report
7	IHC Presentation	3/20/2006	Presentation at IHC showing results to date (i.e. calibration & validation).
8	Land and RFI Quality Control V1.0	5/26/2006	Initial quality control routines that identify and flag RFI and Land Contamination.
9	SST Ingestion Routine	6/30/2006	Initial SST ingestion routine that permits uploading SST tables and inputs SST values into the retrieval algorithm based on latitude-longitude position.
10	Annual Report	6/30/2006	Annual Report